Threshold Photoelectron−Photoion Coincidence Spectroscopy: Dissociation of the 1-Chloroadamantane Ion and the Heat of Formation of the 1-Adamantyl Cation

Yue Li and Tomas Baer*

Department of Chemistry, University of North Carolina, Chapel Hill, North Carolina 27599-3290

Received: August 1, 2001; In Final Form: October 22, 2001

Threshold photoelectron−photoion coincidence spectroscopy was used to investigate the dissociation of the 1-chloroadamantane ion ($C_{10}H_{15}Cl^+$). The product of Cl loss reaction, 1-$C_{10}H_{15}^+$, was the only fragment ion at experimental photon energies below 13.0 eV. Through the simulation of the metastable time-of-flight distributions of the 1-$C_{10}H_{15}^+$ ion and the breakdown diagram, the 0 K appearance energy of 1-$C_{10}H_{15}^+$ was determined to be 10.10 ± 0.02 eV. Using this result and the IE value of 1-$C_{10}H_{15}Cl$, 9.30 ± 0.10 eV, the dissociation energy of the Cl loss reaction was determined to be 0.80 ± 0.10 eV. Using the known heats of formation of $C_{10}H_{15}Cl$ and Cl, the 298 and 0 K heats of formation of the 1-$C_{10}H_{15}^+$ ion were obtained to be 679.2 ± 3.2 and 731.9 ± 3.2 kJ/mol, respectively.

Introduction

Adamantane and its derivatives are the subjects of many theoretical and experimental investigations[1,2] because of their highly symmetrical and rigid structures, which have resulted in their interesting spectroscopic properties[3,4] and wide applications in polymers, pharmaceuticals, and agrochemicals.[5]

The heat of formation of the 1-adamantyl cation (1-$C_{10}H_{15}^+$) has been studied by several experimental and theoretical methods. Experimental techniques used to determine the heat of formation of 1-$C_{10}H_{15}^+$ have included ion−molecule bracketing studies, reaction equilibrium measurements, and appearance energy (AE) measurements. In 1979, Allison and Ridge,[6] studying the halide transfer reactions $Li^+ + 1\text{-}C_{10}H_{15}X \rightarrow LiX + 1\text{-}C_{10}H_{15}^+$ (X = Cl or Br), noted that the reaction is exothermic for the $C_{10}H_{15}Cl$ but not for $C_{10}H_{15}Br$. By assuming values for the heats of formation (some by group additivity) of the other species in the reactions, they determined by bracketing a 1-$C_{10}H_{15}^+$ heat of formation of 672 ± 13 kJ/mol. However, if we use more reliable values for the heats of formation of the 1-$C_{10}H_{15}X$ molecules[7] and the Li^+ ion,[8] we obtain a $\Delta_f H^o_{298K}$[1-$C_{10}H_{15}^+$] of 707 ± 5 kJ/mol. Equilibrium measurements in high-pressure mass spectrometry (HPMS)[9] and ion cyclotron resonance spectroscopy (ICR)[7,10−12] were used to determine the enthalpy and Gibbs energy changes of the hydride or halide transfer reactions between 1-$C_{10}H_{15}X$ (X = H, Cl, or Br) and the *tert*-butyl cation or alkali metal ions. Combining the heats of formation of the other species in the reactions, the heat of formation of 1-$C_{10}H_{15}^+$ can be obtained. Abboud et al.[7] obtained an experimental heat of formation of the 1-adamantyl cation of 684 ± 12 kJ/mol by using the above method combined with a new value[7] for the heat of formation of 1-chloroadamantane. This was in respectable agreement with their theoretical G2 value of 672 ± 10 kJ/mol.[7]

The heat of formation of 1-$C_{10}H_{15}^+$ has also been determined on the basis of several dissociative ionization appearance energy measurements. The AE value of 1-$C_{10}H_{15}^+$ (+ H) from adamantane was measured by photoionization to be 10.6 eV by Fedorova et al.,[13] from which a 298 K heat of formation of 1-$C_{10}H_{15}^+$ of 671 kJ/mol is determined. Similarly, the AE of 1-$C_{10}H_{15}^+$ from $C_{10}H_{15}Br$[14] yields the heat of formation of 1-$C_{10}H_{15}^+$ to be 702 kJ/mol. On the other hand, on the basis of the energy-selected electron ionization AE measurements from several different precursors, Holmes and co-workers[15] determined the heat of formation of 1-$C_{10}H_{15}^+$ to be 636 ± 13 kJ/mol, a result that is substantially lower than the values obtained by the other groups.

To resolve this discrepancy among the various determinations, we embarked on a study to determine the 1-$C_{10}H_{15}^+$ heat of formation by investigating the dissociative ionization onset from 1-chloroadamantane (1-$C_{10}H_{15}Cl$) with threshold photoelectron−photoion coincidence spectroscopy (TPEPICO). This molecule is one of the precursors used by Holmes.[15] By the use of TPEPICO, the molecular ion, 1-$C_{10}H_{15}Cl^+$, can be energy-selected and the dissociation rate constants are measured as a function of the ion internal energy. Because the 1-chloroadamantane ion is a very large ion with a very large density of vibrational states, the measured dissociation onset must take into account the broad thermal energy distribution as well as the slow dissociation rate constants near the dissociation limit.

Experimental Approach

The TPEPICO apparatus has been described in detail previously.[16] Briefly, room-temperature sample vapor was leaked into the experimental chamber through a 1.5 mm diameter inlet and then was ionized with vacuum ultraviolet (VUV) light from an H_2 discharge lamp dispersed by a 1 m normal incidence monochromator. The VUV wavelengths were calibrated using the hydrogen Lyman-α line. Ions and electrons were extracted in opposite directions with an electric field of 20 V/cm. Threshold photoelectrons were selected by a steradiancy analyzer that consists of a flight tube with small apertures that can cut off energetic electrons. Further discrimination against the energetic electrons was provided by a hemispherical electrostatic sector analyzer resulting in a 35 meV combined photon and electron energy resolution. The ions were accelerated to 100 eV in the first 5 cm long acceleration region, and a short second region accelerated the ions to 220 eV. The ions were detected by a multichannel plate after drifting through a 30 cm field-free drift region. The electron and ion signals were used as start

* To whom correspondence should be addressed.

10.1021/jp012962d CCC: $22.00
Published on Web 12/07/2001

and stop pulses for measuring the ion time-of-flight (TOF), respectively, and the TOF for each coincidence event was stored on a multichannel pulse height analyzer. TOF distributions were obtained in 1−48 h depending on the photon intensity and the desired spectrum quality.

Two types of experiments are carried out. First, the fractional abundances of the parent and the daughter ions were measured as a function of the photon energy (breakdown diagram). Second, the product ion TOF distributions were measured at energies close to the dissociation limit of the molecular ion. Slowly dissociating (metastable) ions decay in the first acceleration region. The resulting daughter ion TOF distribution is asymmetrically broadened toward long TOF. The asymmetric peak shapes can be analyzed to extract the ion decay rates as a function of ion internal energy. These two types of data were used together in the data analysis.

The sample of 1-chloroadamantane ($C_{10}H_{15}Cl$, 98%, Aldrich Chemical Co.) was used without further purification.

Quantum Chemical Calculations

In the simulations for the experimental data, reliable vibrational frequencies of the neutral and ionic species are needed to calculate the energy distribution of the molecular ion and reaction rate constants. These were obtained with quantum chemical calculations performed on an Origin 2000 computer at UNC−Chapel Hill using the Gaussian 98 package.[17]

All neutral and ionic species were fully optimized at the DFT (B3LYP)/6-31G* level without symmetry restrictions. The stationary points were confirmed through the calculation of harmonic vibrational frequencies, which also provided the zero point vibrational energies. Because the vibrational frequencies for $C_{10}H_{15}{}^{35}Cl$ and $C_{10}H_{15}{}^{37}Cl$ are nearly identical, we used only a single set for both chlorine isotopes. Figure 1 shows the structures and the main geometrical parameters of neutral and ionic 1-$C_{10}H_{15}Cl$ as well as the 1-$C_{10}H_{15}{}^{+}$ ion. The frequencies obtained by the DFT calculations listed in Table 1 are used in the calculations for the thermal energy distribution and rate constants.

The Cl loss reaction is expected to be a direct dissociation reaction with no exit barrier. Thus, the transition state is not located at a fixed C−Cl bond distance. Its location should be determined by variational transition state theory (VTST).[18−20] Rather than applying this theory here by calculating transition state structures as a function of the C−Cl bond distance, we chose simply to use RRKM theory[18] and to adjust the transition state vibrational frequencies until a good fit with the experiment is observed. However, in our calculation of the $C_{10}H_{15}Cl^{+}$ structure as a function of the C−Cl bond distance, we noticed a stationary point at a C−Cl bond distance of 3.373 Å in which all frequencies are real. This structure, $C_{10}H_{15}Cl^{+}$ (II) in Figure 1, is essentially an ion-induced dipole complex. We thus used its vibrational frequencies as a starting point for fitting the dissociation rate data. The data were modeled by converting the 40 cm^{-1} C−Cl bond stretch frequency into the reaction coordinate (imaginary frequency) and adjusting the other two low-frequency modes. As the $C_{10}H_{15}Cl^{+}$ ion dissociates, these two lowest frequencies will convert into two translational degrees of freedom of the chlorine atom. In the B3LYP calculations for the open-shell species, the spin-squared expectations, $\langle S^2 \rangle$, are close to 0.75, an ideal value for pure spin eingenstates, so that spin contaminations can be ignored.

Results and Discussion

1. Simulation of the TOF Distributions and Breakdown Diagram. The TOF mass spectra of the sample were collected in the photon energy range of 9.7−12.0 eV. Typical TOF distributions obtained at different energies are shown in Figure 2. In this figure, the points correspond to experimental data, whereas the solid lines correspond to the fitted TOF distributions (as discussed in the following section). The ion peaks at 30.1 and 30.26 μs correspond to the parent ions $C_{10}H_{15}{}^{35}Cl^{+}$ (m/z 170) and $C_{10}H_{15}{}^{37}Cl^{+}$ (m/z 172), respectively. In the experimental photon energy range below 13.0 eV, the only fragment ion is $C_{10}H_{15}{}^{+}$ (m/z 135), which corresponds to the following Cl loss reaction product:

$$C_{10}H_{15}Cl^{+} \rightarrow C_{10}H_{15}{}^{+} + Cl^{\bullet} \qquad (1)$$

Figure 2 shows that the parent ion peak consists of two parts, a central sharper peak on top of a broader one. The sharp part results from the effusive jet produced by the sample inlet, whereas the broad peak results from the sample vapor in the background. The simulation calculations indicate that the proportion of the sample from the effusive jet is less than 10%.

The experimental results in Figure 2 show that at photon energies below 10.1 eV the peak shape of the $C_{10}H_{15}{}^{+}$ ion in the TOF mass spectrum is asymmetric, or quasiexponential, thereby indicating a slow dissociation from a metastable parent ion. This asymmetry arises when the product ions are formed during the time the parent ions spend in the acceleration region (about 9.7 μs). The fragment ions that dissociate after exiting the first acceleration region are counted as parent ions. Through analyzing the fragment ion peak shapes, the dissociation rates of the parent ions can be determined. In this analysis, shown as the solid lines in Figure 2, the dissociation rate constant as well as the thermal energy distribution and the resolution function of the electron energy analyzer were taken into account.

The rate constants of the dissociation reaction in eq 1 were calculated using the statistical RRKM theory formula:[18]

$$k(E) = \frac{\sigma N^{\ddagger}(E - E_0)}{h\rho(E)} \qquad (2)$$

in which E_0 is the activation energy, $N^{\ddagger}(E - E_0)$ is the sum of states of the transition state from 0 to $E - E_0$, and $\rho(E)$ is the density of states of the ion. σ is the symmetry parameter, which is 1 for reaction 1.

Because the sample used in the experiments is at room temperature, it has a rather broad thermal energy distribution. As a result, the TPEPICO energy selection produces an ion sample with a thermal energy distribution that results in a distribution of dissociation rate constants. Thus, the modeling of the rate data in Figure 2 was carried out by convoluting the rate constants with the thermal energy distribution.

The internal energy distribution of the molecular ion was calculated with the usual Boltzmann equation

$$P(E) = \frac{\rho(E)\, e^{-E/RT}}{\int_0^{\infty} \rho(E)\, e^{-E/RT}\, dE} \qquad (3)$$

in which the rovibrational density of states, ρ(E), is calculated using a direct count method.[18,21] The 1-chloroadamantane molecule is a symmetric top, and its rotational constants are obtained by the DFT calculations (A = 1.678 GHz, $B = C$ = 0.823 GHz).

The ion energy distribution is also broadened by the electron energy analyzer function. The analyzer function was measured from a threshold photoelectron spectrum (TPES) of acetylene,

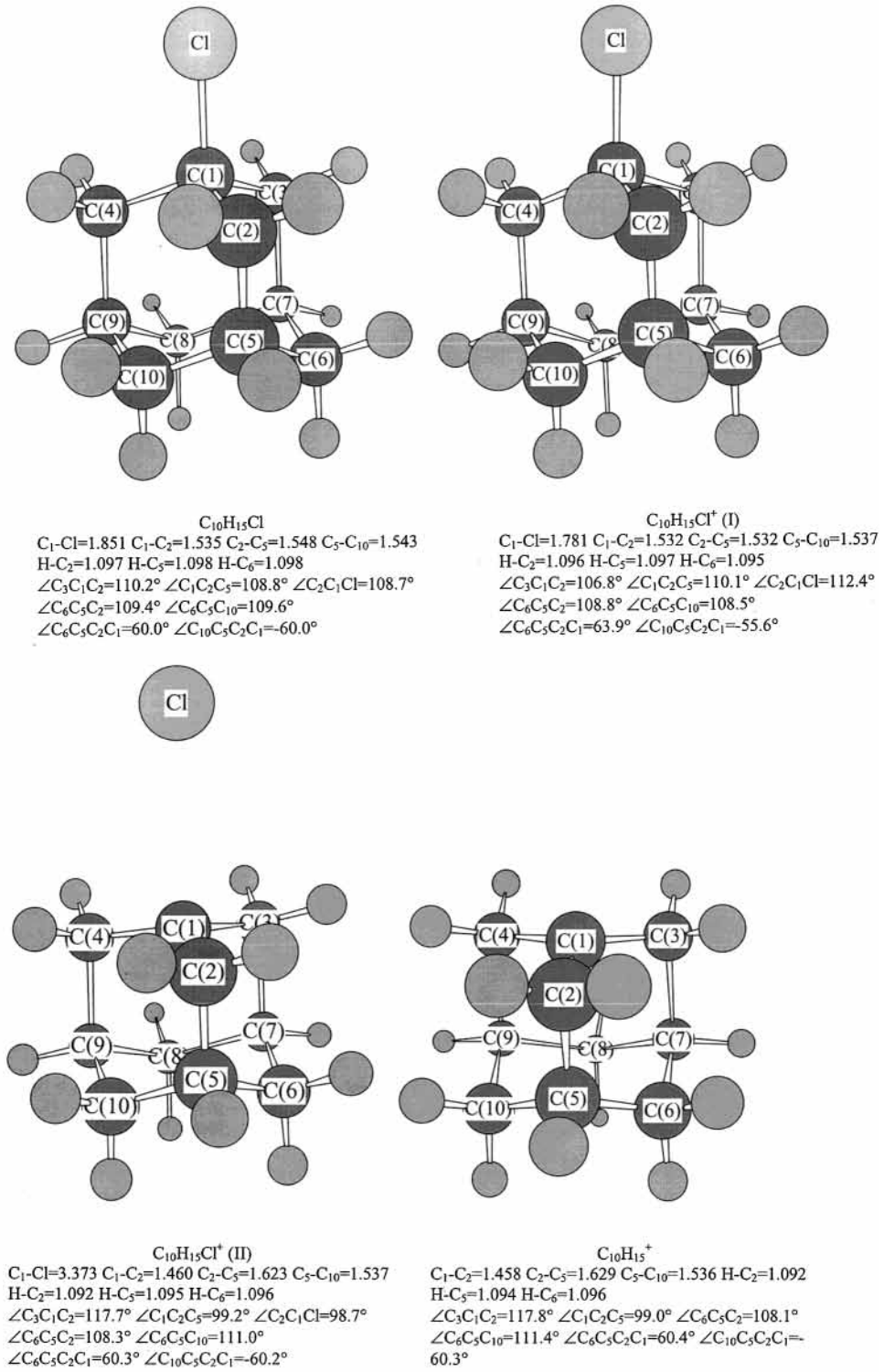

Figure 1. Equilibrium structures and main geometrical parameters obtained at the B3LYP/6-31G* level.

which has widely spaced energy levels. As shown by Sztáray and Baer,[22] this function can be convoluted with the sample thermal energy distribution to yield a total energy broadening function. The thermal energy distribution has an average energy of 185 meV (calculated using the DFT vibrational frequencies), extending over 600 meV, so that the instrumental energy resolution of 35 meV contributed only marginally to the total ion energy distribution.

It is possible, from the data shown in Figure 2, to determine a fractional abundance of parent and product ions as a function of the ion internal energy. Such a ratio, $D^+/(D^++P^+)$ and $P^+/(D^++P^+)$, where D^+ and P^+ are daughter and parent ions, as a function of the ion internal energy constitutes a breakdown diagram. This is shown in Figure 3. The points are the experimental ratios with error estimates, whereas the solid lines are the simulation results, and the vertical dashed line indicates the location of the 0 K dissociation limit of the Cl loss reaction as derived from this simulation.

The ion TOF distributions and the breakdown diagram can be calculated using the following known information: the thermal energy distribution of the molecular ion, the acceleration electric fields, and the acceleration and drift field distances. The

TABLE 1: Frequencies (cm^{-1}) Used in the Energy Distribution and RRKM Calculations

1-$C_{10}H_{15}Cl$	210, 213, 323, 336, 358, 364, 408, 410, 452, 461, 475, 655, 658, 698, 770, 816, 822, 825, 905, 908, 918, 940, 943, 968, 997, 1001, 1052, 1057, 1059, 1060, 1126, 1130, 1132, 1138, 1142, 1216, 1218, 1302, 1304, 1322, 1324, 1324, 1335, 1359, 1360, 1366, 1393, 1395, 1402, 1413, 1415, 1510, 1510, 1523, 1523, 1526, 1548, 3030, 3030, 3031, 3047, 3047, 3051, 3058, 3058, 3066, 3068, 3068, 3073, 3093, 3098, 3099
1-$C_{10}H_{15}Cl^+$	193, 209, 312, 319, 344, 361, 367, 397, 438, 447, 463, 525, 627, 653, 701, 762, 767, 788, 821, 844, 858, 875, 883, 901, 907, 910, 955, 976, 981, 997, 1001, 1048, 1062, 1073, 1106, 1110, 1118, 1158, 1160, 1208, 1213, 1255, 1284, 1292, 1299, 1336, 1347, 1349, 1365, 1379, 1397, 1459, 1470, 1500, 1506, 1512, 1541, 2792, 3026, 3027, 3044, 3060, 3071, 3083, 3086, 3100, 3101, 3104, 3114, 3131, 3135, 3179
TS[a]	−40,[b] 10, 11, 294, 339, 342, 363, 365, 462, 465, 467, 575, 577, 681, 736, 739, 761, 825, 857, 860, 881, 904, 904, 939, 986, 988, 1017, 1028, 1030, 1053, 1093, 1101, 1109, 1109, 1143, 1151, 1153, 1222, 1230, 1231, 1293, 1297, 1298, 1345, 1358, 1359, 1360, 1401, 1401, 1422, 1424, 1503, 1504, 1523, 1537, 1539, 1564, 3067, 3067, 3072, 3102, 3103, 3105, 3106, 3106, 3111, 3112, 3113, 3118, 3173, 3177, 3178
1-$C_{10}H_{15}^+$	293, 337, 339, 361, 362, 463, 464, 468, 570, 571, 678, 728, 730, 766, 830, 855, 857, 882, 903, 903, 940, 988, 989, 1017, 1027, 1028, 1053, 1092, 1100, 1108, 1109, 1144, 1150, 1150, 1224, 1226, 1228, 1292, 1296, 1296, 1342, 1357, 1361, 1362, 1401, 1402, 1423, 1425, 1502, 1503, 1522, 1539, 1542, 1565, 3066, 3066, 3071, 3104, 3104, 3104, 3105, 3106, 3109, 3112, 3112, 3118, 3172, 3177, 3177

[a] The lowest two frequencies were adjusted to fit the experimental results. [b] Reaction coordinate.

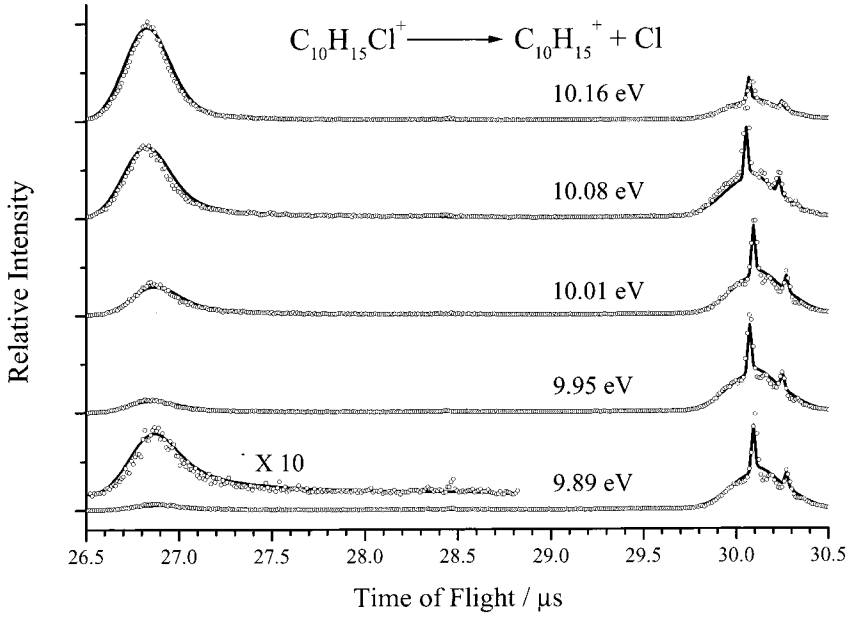

Figure 2. Ion TOF distributions at different photon energies. The points are the experimental data, and the solid lines are the simulation results.

adjustable parameters are the ion dissociation energy and the transition state vibrational frequencies.

By adjusting the energy barrier height and the lowest two frequencies of the transition state, all TOF distributions and the breakdown diagram can be well simulated. The simulation results show that the appearance energy of 1-$C_{10}H_{15}^+$ is 10.10 ± 0.02 eV, in which 0.02 eV is the error limit of this study. Any variance of the AE value beyond this error limit causes the simulated fit to the data to become significantly worse.

Although the determination of the dissociative ionization onset is relatively straightforward because it depends only on well-understood parameters such as the thermal energy distribution, the determination of the adiabatic ionization energy of a large molecule is considerably more difficult. The adiabatic ionization energy is defined as the energy difference between the vibrational and rotational ground states of the molecule and the ion. The PES bands are generally broad because of overlapping absorption peaks from many hot bands between vibrationally and rotationally excited neutral molecules and their corresponding ion states. In principle, it is possible to calculate the shape of the PES band if we know all of the transition probabilities (Franck−Condon factors) connecting the many neutral and ion states. In practice, this information is simply not available or easily calculated. The 1-chloroadamantane vertical and adiabatic ionization energies listed in the NIST Webbook as 9.89 and 9.30 eV, respectively, were determined by Worley et al.[3] This adiabatic IE corresponds to the foot of the PES band. We used it as well as several other values in order to fit the breakdown diagram and the ion TOF distributions. If we raise the value of the adiabatic IE, the rate constants become too large and we can no longer fit the ion fragment ion TOF distribution with its asymmetric tail. Thus, our analysis provides an indirect support for the adiabatic ionization energy reported by Worley et al.[3]

Using the AE result and the adiabatic IE value, the dissociation energy of the C−Cl bond of 1-$C_{10}H_{15}Cl^+$ is obtained to be 0.80 ± 0.10 eV, in which the large error reflects the uncertainty in the adiabatic IE. The RRKM calculated rate curve for reaction 1 is shown in Figure 4. The activation entropy of the dissociation reaction is 31.4 J mol^{-1} K^{-1} at 600 K, a large positive value,

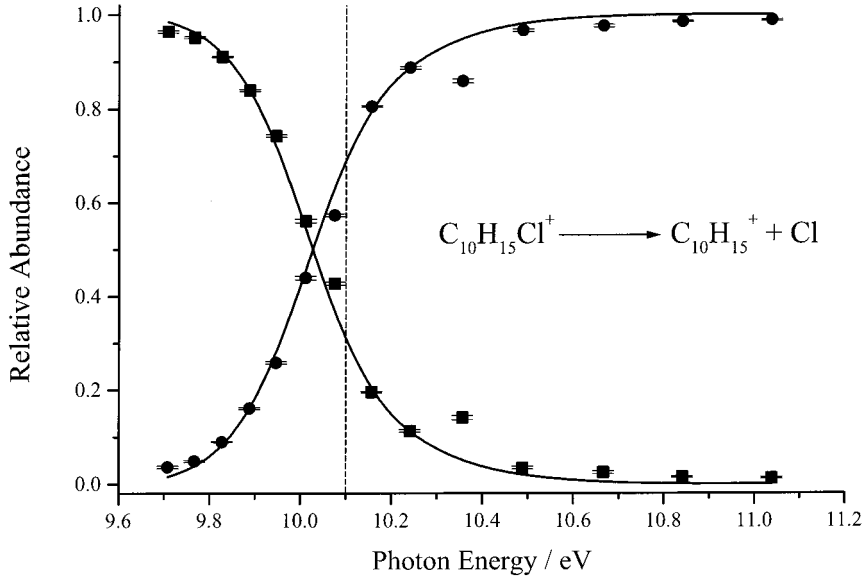

Figure 3. Breakdown diagram of 1-$C_{10}H_{15}Cl^+$. The points are the experimental data with error estimates, and the solid lines are the simulation results. The dashed line indicates the derived 0 K appearance energy of 1-$C_{10}H_{15}^+$.

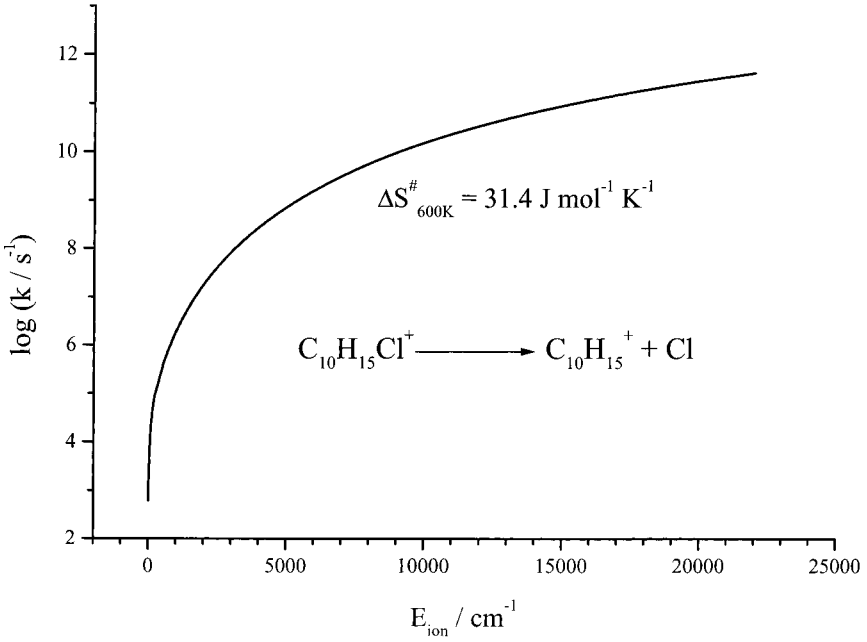

Figure 4. RRKM calculated rate curve of the Cl loss reaction.

which indicates that the dissociation proceeds via a loose transition state. This is further evidence that the reaction is a simple bond-cleavage with no reverse barrier.

2. Thermochemistry. The 298 and 0 K thermochemical data of all relevant molecules and ions are listed in Table 2. The thermochemical values in the table were obtained as follows. The 298 K heat of formation of neutral 1-$C_{10}H_{15}Cl$ was reported to be -177.6 ± 2.5 kJ/mol by Abboud et al.[7] This is an experimental value by combining the standard enthalpy of formation of crystalline 1-chloroadamantane with its standard enthalpy of sublimation. The 298 K heat of formation was converted to a 0 K value of -123.0 ± 2.5 kJ/mol using the following equation:

$$\Delta_f H^o_{0K}[C_{10}H_{15}Cl] = \Delta_f H^o_{298K}[C_{10}H_{15}Cl] - [H^o_{298} - H^o_0][C_{10}H_{15}Cl] + [H^o_{298} - H^o_0][\text{elements}] \quad (4)$$

where the $H^o_{298K} - H^o_{0K}$ function of $C_{10}H_{15}Cl$ was determined using calculated DFT vibrational frequencies and "elements" refers to the sum of the elements in their standard states, i.e., $10C(s) + {}^{15}/_2H_2(g) + {}^1/_2Cl_2(g)$.[27] The 0 K heat of formation of the $C_{10}H_{15}Cl^+$ ion is equal to $\Delta_f H^o_{0K}[C_{10}H_{15}Cl]$ plus the IE of $C_{10}H_{15}Cl$. Using the appearance energy of 1-$C_{10}H_{15}^+$ obtained in this study (10.10 ± 0.02 eV), the 0 K heat of formation of the 1-$C_{10}H_{15}^+$ ion was found to be 731.9 kJ/mol by the equation

$$\Delta_f H^o_{0K}[C_{10}H_{15}^+] = \Delta_f H^o_{0K}[C_{10}H_{15}Cl] + AE - \Delta_f H^o_{0K}[Cl] \quad (5)$$

By a similar approach, $\Delta_f H^o_{298K}[C_{10}H_{15}Cl^+]$ and $\Delta_f H^o_{298K}$-$[C_{10}H_{15}^+]$ can also be determined. Table 2 also lists other available experimental and theoretical results for comparison. Abboud et al.[7] calculated the standard enthalpy and Gibbs energy changes of the hydrogen and chlorine exchange reactions between adamantane, 1-chloroadamantane, and the *tert*-butyl cation using the G2(MP2) technique. The 298 K heat of formation of 1-$C_{10}H_{15}^+$ that they obtained by the G2 calculation

TABLE 2: Thermochemical Results (kJ/mol)[p,q]

species	$\Delta H^o_{f(298K)}$	$\Delta H^o_{f(0K)}$	$H^o_{298K} - H^o_{0K}$	other results of $\Delta H^o_{f(298K)}$
1-$C_{10}H_{15}Cl$	-177.6 ± 2.5[a]	-123.0 ± 2.5[b]	24.01[c]	
1-$C_{10}H_{15}Cl^+$	721 ± 10[d]	774 ± 10[e]	25.62[c]	
1-$C_{10}H_{15}^+$	679.2 ± 3.2[d]	731.9 ± 3.2[f]	21.33[c]	677.8 ± 8.4,[a] 672.4,[g] 707,[h] 665,[i] 680 ± 13,[j] 636 ± 13,[k] 702,[l] 671[m]
1-$C_{10}H_{15}^•$	79.5 ± 4.3[d]	132.7 ± 4.3[n]	20.85[c]	79.5 ± 8.9,[a] 62,[j] 50 ± 13[k]
Cl	121.302[o]	119.621 ± 0.006[o]		

[a] Abboud et al.[7] [b] $\Delta H^o_{298K} \rightarrow \Delta H^o_{0K}$. [c] Determined from the DFT calculated vibrational frequencies. [d] $\Delta H^o_{0K} \rightarrow \Delta H^o_{298K}$. [e] $\Delta H^o_{0K(ion)} = \Delta H^o_{0K(neutral)}$ + IE, and the IE value used in this study is 9.30 ± 0.10 eV (see the text). [f] $\Delta H^o_{0K}(C_{10}H_{15}^+) = \Delta H^o_{0K}(C_{10}H_{15}Cl) + AE - \Delta H^o_{0K}(Cl)$, in which AE is 10.10 ± 0.02 eV. [g] G2 results by Abboud et al.[7] [h] Allison and Ridge,[6] recalculated using the heats of formation that are presently accepted for Li^+, 1-$C_{10}H_{15}Cl$ (1-$C_{10}H_{15}Br$), and LiCl (LiBr). [i] Staley et al.[12] [j] Kruppa and Beauchamp,[26] recalculated using the heats of formation that are presently accepted for adamantane, isobutane, and the *tert*-butyl cation. [k] AE measurements by Holmes and co-workers.[15] [l] AE measurement by Fort.[14] [m] AE measurement by Fedorova et al.[13] [n] $\Delta H^o(C_{10}H_{15}^+) - IE(C_{10}H_{15}^•)$, in which $IE(C_{10}H_{15}^•) = 6.21 \pm 0.03$ eV.[26] [o] NIST-JANAF[8]. [p] In the $H^o_{298K} - H^o_{0K}$ calculations, the heat capacity of electron was treated as 0.0 kJ/mol at all temperatures (the ion convention[23]). To convert to the electron convention, which treats the electron as a real particle, 6.197 kJ/mol should be added to the 298 K heat of formation of each ion. [q] The heat of formation values used in the recalculations are H (218),[24] Li^+ (685.7),[8] Br (111.86),[24] Br^- (−219.0),[8] LiCl (−195.7),[24] LiBr (−153.97),[24] isobutane (−134.9),[24] *tert*-butyl cation (710.9),[24] adamantane (−133.9),[24] and 1-$C_{10}H_{15}Br$ (−131).[25]

is 672.4 kJ/mol. By combining the HPMS experimental results of Kebarle et al.,[9] they also suggested an average value of the experimental and theoretical results, 677.8 ± 8.4 kJ/mol.[7] These results are in good agreement with the 298 K value of 679.2 kJ/mol obtained in this study. The similar thermochemical computation, which is equally based on the experimental results of Kebarle et al., has also been done by Kruppa and Beauchamp.[26] Using the thermochemical values that are presently accepted, the heat of formation of 1-$C_{10}H_{15}^+$ that they obtained is 680 kJ/mol.

Beauchamp et al.[12] obtained an estimate for the R^+-Br^- bond dissociation energy of 1-$C_{10}H_{15}Br$ in the gas phase to be 577 ± 42 kJ/mol using the ion cyclotron resonance technique. Using this energy and the heats of formation of Br^- and 1-$C_{10}H_{15}Br$ (see Table 2), the heat of formation of 1-$C_{10}H_{15}^+$ can be obtained to be 665 kJ/mol, 14 kJ/mol lower than the result obtained in this study. However, no direct experimental result is available for the heat of formation of the 1-$C_{10}H_{15}Br$ precursor, and the GIANT compilation of Lias et al.[25] lists only one estimated value.

The result obtained by Holmes and co-workers,[15] who determined the heat of formation of 1-$C_{10}H_{15}^+$ by the electron ionization AE measurements from several different precursors, is significantly lower than the above results. A possible problem in the electron ionization AE measurements is associated with the accurate determination of the real appearance onsets. This is especially difficult in this case because the sample at room temperature has a broad thermal energy distribution, which will make the real onset shift to a lower energy. It can be seen from the breakdown diagram in Figure 3 that the phenomenological AE value of 1-$C_{10}H_{15}^+$ is about 9.7 eV, which is consistent with the value that Holmes and co-workers measured using the same precursor, 1-$C_{10}H_{15}Cl$. However, the real 0 K onset determined in this study is 10.10 eV, which is 0.4 eV higher than the phenomenological onset.

Using the heat of formation of 1-$C_{10}H_{15}^+$ and the IE value of 1-$C_{10}H_{15}^•$ obtained by Kruppa and Beauchamp,[26] the 0 and 298 K heats of formation of the 1-$C_{10}H_{15}^•$ radical are obtained to be 132.7 ± 4.3 and 79.5 ± 4.3 kJ/mol, respectively. Using this value, the C(tertiary)−H bond dissociation energy in adamantane can be derived to be 431.4 kJ/mol. This value is 30 kJ/mol higher than the corresponding value of isobutene (401.2 kJ/mol).[28] However, the ab initio calculations[7] indicate that these two C−H bonds should have similar bond strengths. Abboud et al.[7] suggested that probable explanation is that the adiabatic ionization energy of the 1-$C_{10}H_{15}^•$ radical may not be well determined. That is, the real IE value should be higher and correspondingly, the heat of formation of the 1-$C_{10}H_{15}^•$ radical is lower; thus, the dissociation energy of the C(tertiary)-H bond in adamantane will become lower, too. The resolution of this problem must await the determination of more accurate adiabatic ionization energies, which as mentioned above, are very difficult to determine.

Conclusions

The Cl loss reaction product ion, 1-$C_{10}H_{15}^+$, was found to be the only fragment ion at photon energies lower than 13.0 eV. The TOF distributions of 1-$C_{10}H_{15}^+$ are asymmetric, which indicates that the parent ion is metastable. From the simulation of these metastable TOF distributions and the breakdown diagram, an accurate 0 K appearance energy of 1-$C_{10}H_{15}^+$ was determined to be 10.10 ± 0.02 eV. Using this result and the adiabatic IE of 1-$C_{10}H_{15}Cl$ (9.30 ± 0.10 eV), the dissociation energy of the C−Cl bond in 1-$C_{10}H_{15}Cl^+$ was determined to be 0.80 ± 0.10 eV. Using the known heats of formation of $C_{10}H_{15}Cl$ and Cl, the 298 and 0 K heats of formation of the 1-$C_{10}H_{15}^+$ ion were obtained to be 679.2 ± 3.2 and 731.9 ± 3.2 kJ/mol, respectively. Using the IE value of 1-$C_{10}H_{15}^•$, the 298 and 0 K heats of formation of 1-$C_{10}H_{15}^•$ were determined to be 79.5 ± 4.3 and 132.7 ± 4.3 kJ/mol, respectively.

References and Notes

(1) Fort R. C. *Adamantane, the Chemistry of Diamond Molecules*; Marcel Dekker: New York, 1976.

(2) Fort, R. C., Jr.; Schleyer, P. v. R. *Chem. Rev.* **1964**, *64*, 277.

(3) Worley, S. D.; Mateescu, G. D.; McFarland, C. W.; Fort, R. C., Jr.; Sheley, C. F. *J. Am. Chem. Soc.* **1973**, *95*, 7580−7586.

(4) Bodor, N.; Dewar, M. J. S.; Worley, S. D. *J. Am. Chem. Soc.* **1970**, *92*, 19−24.

(5) Tominaga, K.; Haga, M. *Chem. Econ. Eng. Rev.* **1986**, *10*, 23.

(6) Allison, J.; Ridge, D. P. *J. Am. Chem. Soc.* **1979**, *101*, 4998−5009.

(7) Flores, H.; Davalos, J. Z.; Abboud, J.-L. M.; Castano, O.; Gomperts, R.; Jimenez, P.; Notario, R.; Roux, M. V. *J. Phys. Chem. A* **1999**, *103*, 7555−7557.

(8) Chase, M. W. *NIST-JANAF Thermochemical Tables*; American Institute of Physics: New York, 1998.

(9) Sharma, R. B.; Sen Sharma, D. K.; Hiraoka, K.; Kebarle, P. *J. Am. Chem. Soc.* **1985**, *107*, 3747−3757.

(10) Abboud, J.-L. M.; Castano, O.; Della, E. W.; Herreros, M.; Muller, P.; Notario, R.; Rossier, J.-C. *J. Am. Chem. Soc.* **1997**, *119*, 2262−2266.

(11) Takeuchi, K.; Takasuka, M.; Shiba, E.; Kinoshita, T.; Okazaki, T.; Abboud, J.-L. M.; Notario, R.; Castano, O. *J. Am. Chem. Soc.* **2000**, *122*, 7351−7357.

(12) Staley, R. H.; Wieting, R. D.; Beauchamp, J. L. *J. Am. Chem. Soc.* **1977**, *99*, 5964−5972.

(13) Fedorova, M. S.; Potapov, V. K.; Denisov, Y. V.; Sorokin, V. V.; Evlasheva, T. I. *Russ. J. Phys. Chem.* **1974**, *48*, 1078−1079.

(14) Fort, R. C., Jr. *Carbonium Ions*; Wiley-Interscience: New York, 1973; Chapter 32, pp 1783−1835.

(15) Aubry, C.; Holmes, J. L.; Walton, J. C. *J. Phys. Chem. A* **1998**, *102*, 1389−1393.

(16) Baer, T.; Booze, J. A.; Weitzel, K. M. *Vacuum ultraviolet photoionization and photodissociation of molecules and clusters*, 1st ed.; World Scientific: Singapore, 1991; Chapter 5, pp 259−298.

(17) Frisch, M. J.; Trucks, G. W.; Schlegel, H. B.; Scuseria, G. E.; Robb, M. A.; Cheeseman, J. R.; Zakrzewski, V. G.; Montgomery, J. A., Jr.; Stratmann, R. E.; Burant, J. C.; Dapprich, S.; Millam, J. M.; Daniels, A. D.; Kudin, K. N.; Strain, M. C.; Farkas, O.; Tomasi, J.; Barone, V.; Cossi, M.; Cammi, R.; Mennucci, B.; Pomelli, C.; Adamo, C.; Clifford, S.; Ochterski, J.; Petersson, G. A.; Ayala, P. Y.; Cui, Q.; Morokuma, K.; Malick, D. K.; Rabuck, A. D.; Raghavachari, K.; Foresman, J. B.; Cioslowski, J.; Ortiz, J. V.; Stefanov, B. B.; Liu, G.; Liashenko, A.; Piskorz, P.; Komaromi, I.; Gomperts, R.; Martin, R. L.; Fox, D. J.; Keith, T.; Al-Laham, M. A.; Peng, C. Y.; Nanayakkara, A.; Gonzalez, C.; Challacombe, M.; Gill, P. M. W.; Johnson, B. G.; Chen, W.; Wong, M. W.; Andres, J. L.; Head-Gordon, M.; Replogle, E. S.; Pople, J. A. *Gaussian 98*, revision A.7; Gaussian, Inc.: Pittsburgh, PA, 1998.

(18) Baer, T.; Hase, W. L. *Unimolecular Reaction Dynamics: Theory and Experiments*; Oxford University Press: New York, 1996.

(19) Wardlaw, D. M.; Marcus, R. A. *Adv. Chem. Phys.* **1988**, *70*, 231−263.

(20) Hase, W. L. *Chem. Phys. Lett.* **1987**, *139*, 389−394.

(21) Beyer, T.; Swinehart, D. R. *ACM Commun.* **1973**, *16*, 379.

(22) Sztaray, B.; Baer, T. *J. Am. Chem. Soc.* **2000**, *122*, 9219−9226.

(23) Rosenstock, H. M.; Draxl, K.; Steiner, B. W.; Herron, J. T. *J. Phys. Chem. Ref. Data* **1977**, *6*.

(24) http://webbook.nist.gov/chemistry/om/.

(25) Lias, S. G.; Bartmess, J. E.; Liebman, J. F.; Holmes, J. L.; Levin, R. D.; Mallard, W. G. *Gas-Phase Ion and Neutral Thermochemistry, J. Phys. Chem. Ref. Data Vol 17, suppl. 1*; NSRDS, U.S. Government Printing Office: Washington, DC, 1988.

(26) Kruppa, G. H.; Beauchamp, J. L. *J. Am. Chem. Soc.* **1986**, *108*, 2162−2169.

(27) Wagman, D. D.; Evans, W. H. E.; Parker, V. B.; Schum, R. H.; Halow, I.; Mailey, S. M.; Churney, K. L.; Nuttall, R. L. *The NBS Tables of Chemical Thermodynamic Properties, J. Phys. Chem. Ref. Data Vol. 11 Suppl. 2*; NSRDS, U.S. Government Printing Office; Washington, DC, 1982.

(28) Gutman, D. *Acc. Chem. Res.* **1990**, *23*, 375−380.